Sensorless Vector Control of Linear Induction Motor on Primary and Secondary Flux Oriented based on Fuzzy PI Controller

Mohammad Sarvi[1], Hassan Zamani [2]

[1] Faculty of Technical & Engineering, Imam Khomeini International University Qazvin, Iran. Email: sarvi@eng.ikiu.ac.ir
[2] Faculty of Technical & Engineering, sImam Khomeini International University Qazvin, Iran. Email: zamani.4566@gmail.com

Abstract

This paper presents a sensorless system drive on primary flux oriented control (PFOC) and secondary flux oriented control (SFOC) for the linear induction motor (LIM) with taking into account end effect. Extended kalman filter (EKF) is applied to estimate LIM speed by measuring motor voltages and currents. In order to achieve desirable dynamic and robustness motor performance instead of traditional PI controller, a fuzzy PI controller is used for speed regulation in LIM vector control. The accuracy and validity of fuzzy PI controller operation are investigated and evaluated and its results are compared with traditional PI controller. Transient and steady state responses of proposed controller under load thrust variations and speed command are studied. Also characteristics and performances of primary flux oriented control (PFOC) and secondary flux oriented control (SFOC) for the linear induction motor are compared with each other. In order to evaluate the proposed method, simulations are performed in MATLAB/SIMULINK. Results show that the fuzzy PI controller has more excellent performance than the traditional PI controller and also PFOC has better performance than SFOC, because SFOC depend on rotor resistance. EKF properly estimate motor speed by measuring motor voltages and currents and therefore speed sensor can be eliminated.

Keywords: Linear Induction Motor; Vector Control; Fuzzy PI Controller; Extended Kalman Filter; Primary Flux Oriented; Secondary Flux Oriented.

1. Introduction

In recent years, linear induction motors (LIMs) due to their high starting thrust, low mechanical losses, no need to gear for motion and low size of motor are utilized in a wide range of applications such as urban transient systems, robotic machines, elevators, sliding doors and so on [1-2]. In these types of motors, the moving and stationary sections are nominated primary and secondary, respectively. Primary voltages and currents produce a magnetic field that moves along the primary. This field will lead to excite current and magnetic field in the secondary. Interaction of these two fields will generate motivation thrust [3]. One of the most famous and effective methods in control of the ac machines for achieving high dynamic performance is vector control strategy. The vector control techniques are usually referred to field-oriented control (FOC). The basic idea of the FOC algorithm is to decouple flux from the thrust. As a result both components can be controlled separately after separation. For decoupling, reference frame can be aligned with primary or secondary flux [4-5]. Each of these methods has advantages and disadvantages that were presented in [6-9].

A problem in vector control either in primary or in secondary reference frame is their controllers. The traditional PI controller in vector control has disadvantages such as need to precise mathematic system's model and adjustment of its coefficients, while intelligent control methods like fuzzy PI controller are self-adjustment and insensitive to parameters variations, therefore their response are

very robust [10-12]. For closed loop speed control of LIM, having precise knowledge about linear speed is necessary. The usual position sensors like resolvers and optical encoders lead to both increasing cost and decreasing reliability of the system. With considering of these drawbacks, sensorless methods can be used. For sensorless control of system, different algorithms such as algorithms based on the back electromotive force (BEMF), model reference adaptive system (MRAS) and state observer have been proposed [13, 14]. The BEMF method is useless in low speed condition because the induced voltage in comparison with the noise is too small. Also the MRAS method cannot have good performance in low speed, because MRAS is greatly depended on the accuracy of the motor model. The extended kalman filter (EKF) as state observer is an extended form of the kalman filter and estimates dynamic states of nonlinear system by numeric iteration methods. This filter due to maintain estimations of past, present, and future states is very powerful and has high performance in over speed range even in condition that there aren't precise recognition of system parameters and measurements are mixed with noise [15, 16]. Therefore EKF for closed loop speed control of LIM is a suitable option.

In this paper, indirect vector control for LIM based on primary and secondary flux oriented has been developed and their performances are investigated and also compared with each other. Also a fuzzy PI controller is designed and their characteristics are compared with conventional PI controller. Furthermore EKF estimator is presented for LIM speed estimation. This paper is organized as follow: In section 2, dynamic model of LIM is presented. Optimal EKF algorithm is described in section 3. In section 4 the vector control for LIM is presented. Fuzzy PI controller is designed in section 5. In section 6 simulation results and their analyses are presented. Conclusions of this paper are presented in section 7.Method

2. Dynamic Model of LIM

The dynamic model of LIM is analysed by using the dq model of the equivalent electrical circuit with considering end-effect. With moving the LIM, both appearing and disappearing of the field in entrance and exit parts of the machine lead to yield the eddy current in the secondary sheet. The eddy current effect can be determined by modifying of magnetization inductance of the d-axis equivalent electrical circuit. [3]

Fig.1 shows the qd model of the equivalent electrical circuit with end-effect. From this model, the primary and secondary voltage equations in the synchronous reference frame are given by: [17]

$$V_{qx} = R_x i_{qx} + \frac{d}{dt}\lambda_{qx} + \omega_e \lambda_{dx} \tag{1}$$

$$V_{dx} = R_x i_{dx} + R_y f(Q)\big(i_{dx} + i_{dy}\big) + \frac{d}{dt}\lambda_{dx} - \omega_e \lambda_{qx} \tag{2}$$

$$0 = R_y i_{qy} + \frac{d}{dt}\lambda_{qy} + \big(\omega_e - \omega_y\big)\lambda_{dy} \tag{3}$$

$$0 = R_y i_{dy} + R_y f(Q)\big(i_{dx} + i_{dy}\big) + \frac{d}{dt}\lambda_{dy} - (\omega_e - \omega_y)\lambda_{qy} \tag{4}$$

Where:

$$\lambda_{qx} = L_x i_{qx} + L_m i_{qy} \tag{5}$$

$$\lambda_{dx} = L'_x i_{dx} + L'_m i_{dy} \tag{6}$$

$$\lambda_{qy} = L_y i_{qy} + L_m i_{qx} \tag{7}$$

$$\lambda_{dy} = L'_y i_{dy} + L'_m i_{dx} \tag{8}$$

$$L_x = L_{lx} + L_m \tag{9}$$

$$L_y = L_{ly} + L_m \tag{10}$$

$$L'_m = L_m\big(1 - f(Q)\big) \tag{11}$$

$$L'_x = L_{lx} + L'_m \tag{12}$$

$$L'_y = L_{ly} + L'_m \tag{13}$$

$$f(Q) = \frac{1 - e^{-Q}}{Q} \tag{14}$$

$$Q = \frac{DR_r}{\big(L_{ly} + L_m\big)v} \tag{15}$$

Where the relation between linear speed and angular speed in LIM can be written as following:

$$\omega = \frac{\pi}{\tau_p} v \tag{16}$$

Q in above equations is a factor related to primary length and speed for evaluating end-effect. According to Q factor, in low speed condition, end-effect can be neglected. Therefore in low speed there isn't any change in flux and magnetization inductance. On the contrary, with increasing speed, end-effect will be stronger more and will reduce flux and magnetization inductance of the LIM.

For modeling of eddy current losses, a resistance is inserted in series with the inductance $L_m[1 - f(Q)]$ in the magnetization branch of the d-axis equivalent circuit. Eddy current losses can be represented by $R_y f(Q)$. The thrust force is given by: [17]

$$F_e = \frac{3\pi}{2\tau_p}\frac{p}{2}\left(\lambda_{dx} i_{qx} - \lambda_{qx} i_{dx}\right) \quad (17)$$

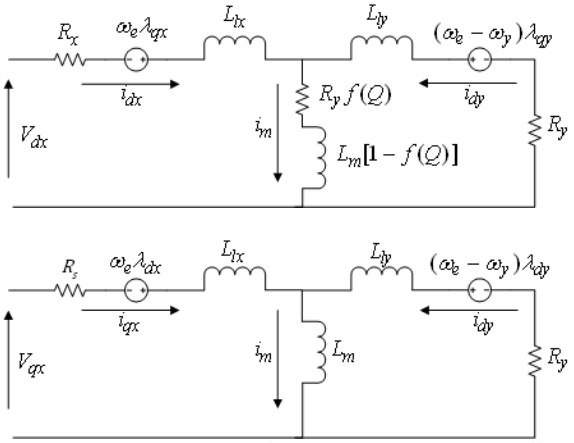

Fig.1. The equivalent circuit of the LIM including the end-effect; (a) d-axis equivalent circuit, (b) q-axis equivalent circuit.

3. Optimal EKF Algorithm

The kalman filter (KF) algorithm as an observer, tries to estimate states of control system that is defined by linear differential equations. Therefore in order to implement the KF algorithm in nonlinear system, equations must be linear. A kalman filter that uses linear equation is referred to as an extended kalman filter or EKF [16]. The primary and secondary voltages and currents equations on synchronous reference frame can be expressed in state space form as follows:

$$\frac{d}{dt}\lambda_{qy} = \frac{R_y L_m}{\Delta}\lambda_{qx} - \frac{R_y L_x}{\Delta}\lambda_{qy} - \omega_{sl}\lambda_{dy} \quad (18)$$

$$\frac{d}{dt}\lambda_{dy} = \left[\frac{R_y(1+f)L'_m}{\Delta} - \frac{R_y f L'_y}{\Delta'}\right]\lambda_{dx} + \omega_{sl}\lambda_{qy} + \left[\frac{R_y f L'_m}{\Delta'} - \frac{R_y(1+f)L'_x}{\Delta'}\right]\lambda_{dy} \quad (19)$$

$$\frac{d}{dt}\lambda_{qx} = V_{qx} - \frac{R_x L_y}{\Delta}\lambda_{qx} + \frac{R_x L_m}{\Delta}\lambda_{qy} - \omega_e\lambda_{dx} \quad (20)$$

$$\frac{d}{dt}\lambda_{dx} = V_{dx} + \omega_e\lambda_{qx} + \left[\frac{R_y f L'_m}{\Delta'} - \frac{R_x + R_y f}{\Delta'}\right]\lambda_{dx} + \left[\frac{(R_x + R_y f)L'_m - R_y f L'_x}{\Delta'}\right]\lambda_{dy} \quad (21)$$

Where

$$\Delta = L_x L_y - L_m^2 \quad (22)$$

$$\Delta' = L'_x L'_y - L^2_{m'} \quad (23)$$

The mechanical dynamic equation of motor is:

$$\frac{d}{dt}v = \frac{1}{M}(F_e - F_l) \quad (24)$$

The state equations of the LIM are given as:

$$x(k+1) = x(k) + T_s.\left[f\big(x(k)\big) + Bu(k)\right] \quad (25)$$

$$y(k) = h\big(x(k)\big) \quad (26)$$

The f, B, u and h are given in appendix A. Also T_s is sampling period time. The state variables and output vectors are as following:

$$x(k) = \left[\lambda_{qx}(k)\ \lambda_{dx}(k)\ \lambda_{qy}(k)\ \lambda_{dy}(k)\ v(k)\right]^T \quad (27)$$

$$y(k) = \left[i_{qx}(k)\ i_{dx}(k)\right]^T \quad (28)$$

The linear and discrete equations of LIM are given as following:

$$x(k+1) = x(k) + T_s.\left[F(x(k)) + Bu(k) + \rho(k)\right] \quad (29)$$

$$y(k) = Hx(k) + r(k) \quad (30)$$

F and H factors are linearization of f and h and their values are given in appendix A. ρ(k) and r(k) are zero-mean white Gaussian noises with covariance Q and R respectively. The system noise ρ(k) take into consideration the system disturbances and model inaccuracy, while r(k) represent the measurement noise. The discrete optimal EKF equation is given by:

a. Predict step:

$$x(k+1) = x(k) + T_s\left[f\big(x(k)\big) + Bu(k)\right] \quad (31)$$

$$P(k+1) = F(k)P(k) + P(k)F^T(k) + Q - K(k)RK^T(k) \quad (32)$$

b. Predict step:

$$K(k) = P(k)H^T R^{-1} \quad (33)$$

$$x(k+1) = x(k) + K(k)[(y(k) - Hx(k)] \qquad (34)$$

By computing only the lower triangular form of the symmetric matrixes (P, K) and considering zero array in F matrix, the volume and time of computation can be reduced.

4. Vector Control of LIM

The vector control scheme for LIM can be analysed in the same way as for rotational induction motor. The fundamental difference between them is existence of speed-dependent resistance and inductance in the d-axis branch which makes difficult decoupling of flux and thrust in LIM.

4.1. Primary Flux Oriented Control

With using Eq. (3) to (8) and after some mathematical manipulation of the machine equations, and with considering $\lambda_{qx} = 0$ and $\lambda_{dx} = \lambda_x$, the slip angular speed, flux and thrust in PFOC are determined as following:

$$\omega_{sl} = \frac{\frac{R_y L_x}{L_m} i_{qx}}{\frac{L'_y}{L'_m}\lambda_{dx} + \left(L'_m - \frac{L'_y L'_x}{L'_m}\right) i_{dx}} \qquad (35)$$

$$\lambda_{dx}\frac{R_y(1+f(Q))}{L'_m} = \left[\frac{L'_x R_y(1+f(Q))}{L'_m} - R_y f(Q)\right] i_{dx} + \left[L_m - \frac{L_y L_x}{L_m}\right]\omega_{sl} i_{qx} \qquad (36)$$

$$F_e = \frac{3}{2}\frac{\pi}{\tau_p}\frac{P}{2}\left(\lambda_{dx} i_{qx}\right) \qquad (37)$$

The main aim in vector control is to decouple flux and thrust. Eqs. (36) and (37) show that the primary flux is not only proportional to i_{dx} but also is proportional to i_{qx} and so there is a coupling between flux and thrust. Hence for overcome to this problem, the d-axis current should be compensated. The compensator component in PFOC can be determined by:

$$i_{dx(componsate)} = \frac{\omega_{sl}\left(\frac{L_y L_x}{L_m} - L_m\right)}{\frac{L'_x R_y(1+f(Q))}{L'_m}} i_{qx} \qquad (38)$$

The block diagram of vector control for LIM based on PFOC scheme is given in Fig. 2.

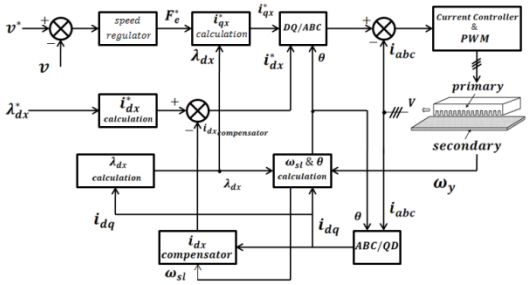

Fig.2. Block diagram of vector-control for LIM based on PFOC.

4.2. Secondary Flux Oriented Control

With using Eqs. (3), (4), (7) and (8) and after some mathematical manipulation of the machine equations and with considering $\lambda_{qy} = 0$ and $\lambda_{dy} = \lambda_y$, the slip angular speed, flux and thrust in SFOC are determined as following:

$$\omega_{sl} = \frac{R_y}{L_y}\frac{L_m}{\lambda_{dy}} i_{qx} \qquad (39)$$

$$\lambda_{dy} = \frac{\left(L'_m - R_y f(Q)\right) L'_y}{R_y\left(1+f(Q)\right)} i_{dx} \qquad (40)$$

$$F_e = \frac{3}{2}\frac{\pi}{\tau_p}\frac{P}{2}\frac{L'_m}{L'_y}\left[\lambda_{dy} i_{qx} - \frac{L_{ly}^2 f(Q)}{L_y(1-f(Q))} i_{dx} i_{qx}\right] = k\left[\lambda_{dy} i_{qx} - \frac{L_{ly}^2 f(Q)}{L_y(1-f(Q))} i_{dx} i_{qx}\right] \qquad (41)$$

Eq. (41) shows that the thrust is not only proportional to i_{qx} but also is proportional to i_{dx} and so there is a coupling between flux and thrust. Hence for overcome to this problem, the q-axis current should be compensated. The compensator component in SFOC can be determined by:

$$i_{qx(componsate)} = \frac{\frac{L_{ly}^2 f(Q)}{L_y\left(1-f(Q)\right)} i_{dx} i_{qx}}{\lambda_{dy}} \qquad (42)$$

The block diagram of LIM vector control based on SFOC scheme is given in Fig. 3.

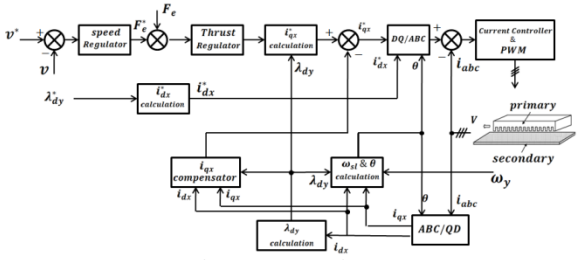

Fig.3. Block diagram of vector-control for LIM based on SFOC.

5. Design of Fuzzy PI Controller

Fuzzy logic has been widely applied in power electronic systems, off line PI and PID tuning, nonlinearity compensation, online and offline diagnostics optimization of drive systems based on online search and so on. In this section for achieving a stable system with appropriate settling time and no overshoot, a fuzzy PI controller is used. Fig. 4 demonstrates structure of a fuzzy PI controller for regulation of speed for LIM. This controller has two inputs and one output. The inputs are speed error (E) and change in speed error (CE) and the output of this controller (U) is electromagnetic thrust. The fuzzification and defuzzification are triangular and centroid, respectively. Also applied inference engine is Mamdani. There are seven memberships functions for E and CE signals whereas there are nine memberships functions for U. Table 1 shows the corresponding rule for fuzzy PI controller, where (NVB) is negative very big, (NB) is negative big, (NM) negative middle, (NS) negative small, (Z) zero, (PS) positive small, (PM) positive middle, (PB) positive big and (PVB) is positive very big [18]. For more comprehension of fuzzy PI controller rule, considering a simple PI controller in following equation:

$$DU = k_1 E + k_2 CE \tag{43}$$

Where k_1 and k_2 are constant factors in a simple PI controller and are nonlinear in fuzzy PI controller. According to Eq. (43), a fuzzy control algorithm for PI controller can be written as table 1. A sample fuzzy rule is as following:

if E = positive small (PS) and CE = zero then DU =positive small (PS)

Finally, it should be considered that the output of fuzzy PI controller is integral of DU. Functional block diagram of fuzzy PI controller in MATLAB is illustrated in Fig. 5.

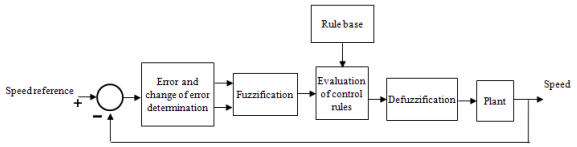

Fig.4. Structure of a fuzzy PI controller.

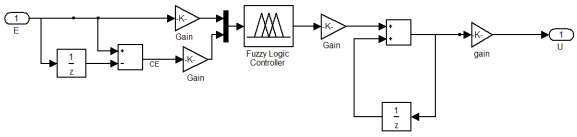

Fig.5. Functional block diagram of fuzzy PI controller.

6. Simulation Results

In this section, the results of overall system drive for LIM with each of the vector control strategies as well as results of EKF sensorless vector control are presented. All simulations are done in MATLAB/SIMULINK software. The motor and EKF are modeled by using S-Function and for simulation of fuzzy PI controller, MATLAB toolbox is used. The LIM parameters used in this simulation are given in table 2. For all of the simulations, primary and secondary fluxes are considered equal to 0.5 Wb.

Table.1
Fuzzy rules table.

CE \ E	NB	NM	NS	Z	PS	PM	PB
NB	NVB	NVB	NVB	NB	NM	NS	Z
NM	NVB	NVB	NB	NM	NS	Z	PS
NS	NVB	NB	NM	NS	Z	PS	PM
Z	NB	NM	NS	Z	PS	PM	PB
PS	NM	NS	Z	PS	PM	PB	PVB
PM	NS	Z	PS	PM	PB	PVB	PVB
PB	Z	PS	PM	PB	PVB	PVB	PVB

Table.2
Specifications of used LIM in the simulation.

Parameters	Value
Primary length	0.286 (m)
Number of poles	2
Pole pitch	0.066 (m)
Primary resistance	1.25 (Ω)
secondary resistance	2.7 (Ω)
Primary leakage inductance	0.0075 (H)
Secondary leakage inductance	0.0005 (H)
Magnetizing inductance	0.0326 (H)
Mass	50 (Kg)

6.1. Comparison of PI and Fuzzy PI Controllers in PFOC

Fig. 6 shows the performance of the simulated LIM vector control with PFOC method for PI and fuzzy PI controller when speed command changes at

t=0.25 s from 4 m/s to 7 m/s. Figs. 7 and 8 show speed and thrust responses of the system for thrust command step, respectively, where speed command is fixed in 5m/s and thrust changes at t=0.25 s from zero to 1000 N.

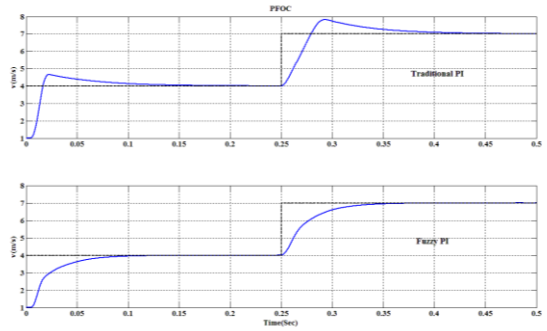

Fig.6. The speed response on PFOC for traditional PI and fuzzy PI controllers with *F*=0 N for speed command changing from 4 m/s to 7 m/s.

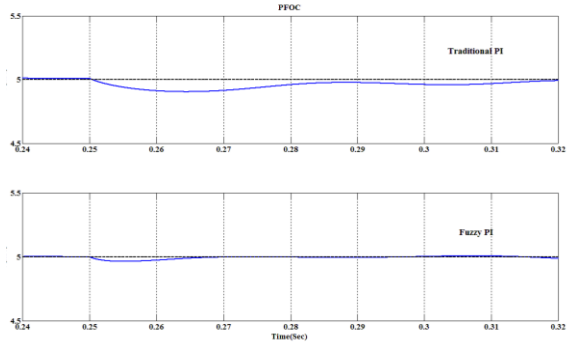

Fig.7. The speed response on PFOC for traditional PI and fuzzy PI controllers with *V*= 5 m/s for thrust command changing from 0 N to 1000 N.

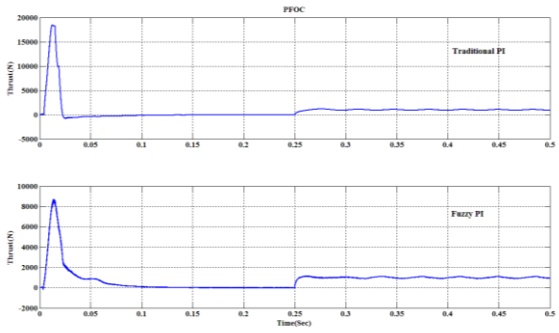

Fig.8. The thrust response on PFOC for traditional PI and fuzzy PI controllers with *V*=5 m/s for thrust command changing from 0 N to 1000 N.

6.2. Comparison of PI and Fuzzy PI Controllers in SFOC

Fig. 9 shows the performance of the implement LIM vector control in SFOC method for PI and fuzzy PI controller when speed command changes at t=0.25 s from 4 m/s to 7 m/s. Figs. 10 and 11 show speed and thrust responses of the system for thrust command step, respectively, where speed command is fixed in 5 m/s and thrust changes at t=0.25 s from 0 N to 1000 N. The results of the speed response in Figs. 6 and 9 are given in table 3. These results clearly demonstrate that speed regulators based on the fuzzy PI have higher performance (lower settling time and zero overshoot for speed response) than traditional PI.

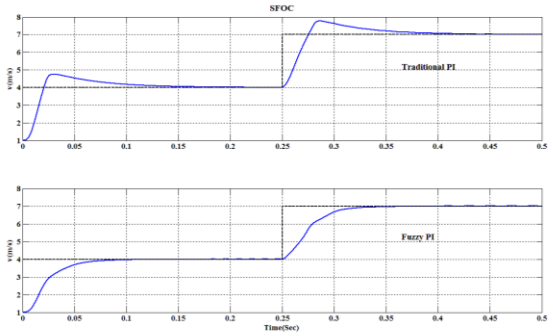

Fig.9. The speed response on SFOC for traditional PI and fuzzy PI controllers with *F*=0 N for speed command changing from 4 m/s to 7 m/s.

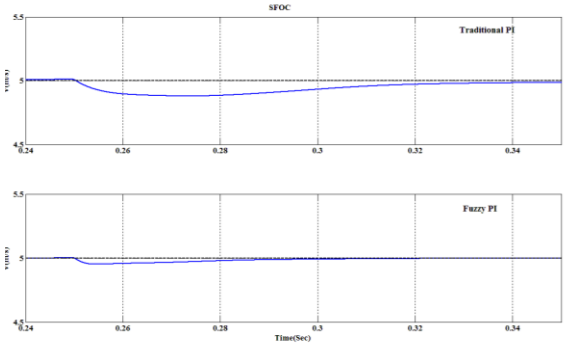

Fig.10. The speed response on SFOC for traditional PI and fuzzy PI controllers with *V*=5 m/s for thrust command changing from 0 N to 1000 N.

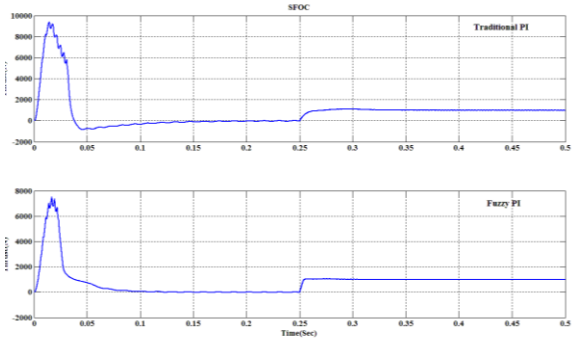

Fig.11. The thrust response on SFOC for traditional PI and fuzzy PI controllers with *V*=5 m/s for thrust command changing from 0 N to 1000 N.

6.3. The Sensitivity to Applied Thrust and Secondary Resistance Variations in PFOC and SFOC

In this case after applying thrust equal to 1000 N at t=0.25 s, the secondary resistance is varied at t=0.35 s and t=0.45 s to 1 Ω and 10 Ω, respectively. Also speed is 5m/s in these conditions. Figs. 12-13 and table 4 show the speed response for these changes. In table 4, overshoot and undershoot values are presented with positive and negative signs, respectively. These results demonstrate that presented PI fuzzy controller has robust performance in comparison with traditional PI. Also vector control in PFOC has better performance than vector control in SFOC, because PFOC is independent from secondary resistance.

6.4. Results of Sensorless Vector Control

Figs. 14 and 15 show the results of sensorless SFOC based on fuzzy PI controller. In this study for investigation of EKF performance, 20% noise is added to motor current. Also sensorless PFOC was investigated and simulated, and its results are confirmed the EKF excellent performance. The results show, estimation of speed by EKF is very accurate despite of noise existence in system.

7. Conclusion

The dynamic model of LIM by considering end-effect is studied and the vector control based on PFOC and SFOC methods with traditional PI and fuzzy PI controller have been discussed and analysed. Then sensorless vector control for each of two schemes (PFOC and SFOC) based on EKF has been studied. Simulation results show that fuzzy PI controller has fast and precise speed response in compare with PI controller. The results demonstrate that intelligent controllers have robustness performance. The results show that vector control in PFOC has better performance than vector control in SFOC, because PFOC is independent from secondary resistance. Also in sensorless control, the estimations and actual values results confirm excellent tracking performance of the EKF in motor speed in SFOC and PFOC.

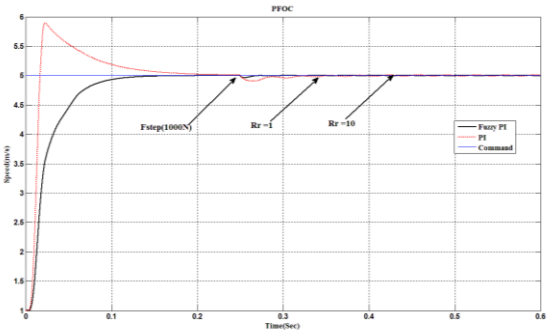

Fig.12. The speed response on PFOC for traditional PI and fuzzy PI controller with *V*=5 m/s for thrust and parameter variations.

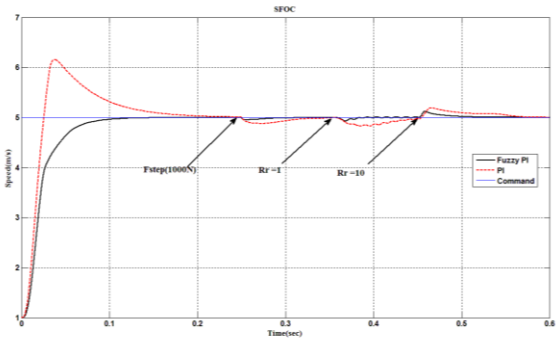

Fig.13. The speed response on SFOC for traditional PI and fuzzy PI controller with *V*=5 m/s for thrust and parameter variations.

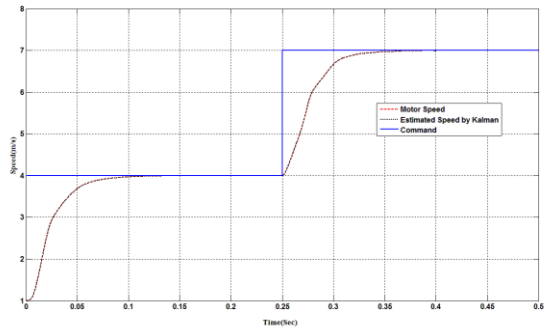

Fig.14. The speed response of sensorless SFOC based on fuzzy PI controller for speed command changing from 4 m/s to 7 m/s.

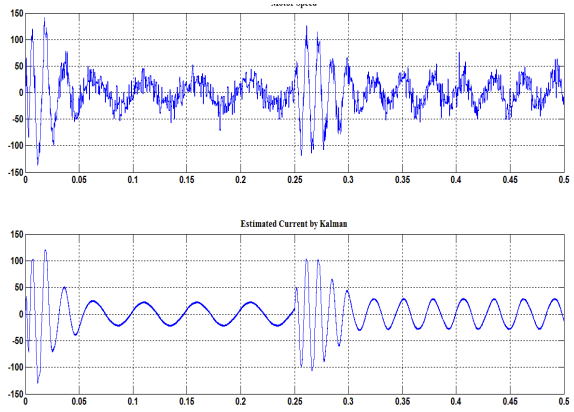

Fig.15. The motor current for SFOC; (a) actual current, (b) estimated current with EKF.

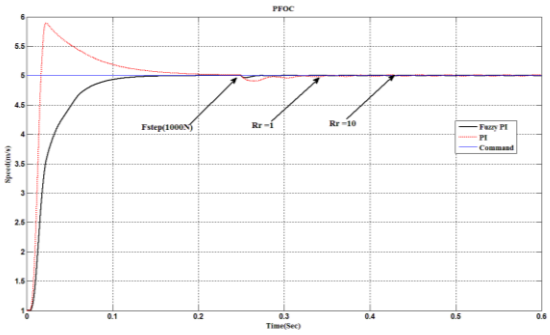

Table.3
Results of the speed response.

Control strategy	Overshoot (%)		Settling time (S)	
PFOC with traditional PI controller	0 to 4 m/s	4m/s to 7 m/s	0 to 4 m/s	4m/s to 7 m/s
PFOC with fuzzy PI controller	16.57	11.61	0.18	0.45
SFOC with traditional PI controller	0	0	0.13	0.39
SFOC with fuzzy PI controller	18.77	10.86	0.19	0.46
SFOC with fuzzy PI controller	0	0	0.15	0.4

Table.4
Results of the speed response.

Control strategy	Undershoot with applied thrust (%)	Undershoot & overshoot with variable parameter	
	F_l = 1000 N	R_r= 1 Ω	R_r= 10 Ω
PFOC with traditional PI controller	-2	-0.8	0
PFOC with fuzzy PI controller	-1.52	0	0
SFOC with traditional PI controller	-2.36	-3.22	+1.74
SFOC with fuzzy PI controller	-1.8	-3.8	+2.3

Nomenclature:

V_{qx} Quadrature axis primary voltage (V)
V_{dx} Direct axis primary voltage (V)
i_{qx} Quadrature axis primary current (A)
i_{dx} Direct axis primary current (A)
i_{qy} Quadrature axis secondary current (A)
i_{dy} Direct axis secondary current (A)
λ_{qx} Quadrature axis primary flux (wb)
λ_{dx} Direct axis primary flux (Wb)
λ_{qy} Quadrature axis secondary flux (Wb)
λ_{dy} Direct axis secondary flux (wb)
R_x Primary resistance (Ω)
R_y Secondary resistance (Ω)
L_{lx} Primary leakage inductance (H)
L_{ly} Secondary leakage inductance (H)
L_m Magnetizing inductance (H)
τ_p Pole pitch (m)
D Primary length (m)
P **Number of machine poles**

Appendix A

$$k_t = \frac{3}{M^2}\frac{\pi^2}{\tau_p^2} \tag{44}$$

$$A_{25} = \frac{\{[R_y(L_m' - L_y')df - R_x df]\lambda_{dx} + [R_y(L_m' - L_x')df + R_x dL]\lambda_{dy}\}\Delta'}{\Delta'^2} + \frac{-\{[R_y f L_m' - (R_s + R_r f)L_r'] * \lambda_{dx} + [(R_x + R_r f)L_m' - R_r f L_s']\}d\Delta'}{\Delta'^2} \tag{45}$$

$$A_{45} = \frac{\{[R_y(L_m' - L_y')df + R_y dL]\lambda_{dx} + [R_r(L_m' - L_s')df - R_r dL]\lambda_{dy}\}\Delta'}{\Delta'^2} + \frac{\{[R_r(1+f)L_m' - R_r f L_y']\lambda_{dx} + [R_y f L_m' - R_r(1+f)L_x']\lambda_{dy}\}d\Delta'}{\Delta'^2} \tag{46}$$

$$A_{55} = \frac{[L_y' * d\Delta' - \Delta' dL]\lambda_{dx}\lambda_{qx} + [\Delta' dL - L_m' d\Delta']\lambda_{qx}\lambda_{dr}}{\Delta'^2} \tag{47}$$

$$C_{25} = \frac{[\Delta' d\Delta - L_r' d\Delta']\lambda_{dx} - [\Delta' dL - d\Delta' L_m']\lambda_{dy}}{\Delta'^2} \tag{48}$$

$$f = \begin{bmatrix} V_{qx} - \frac{R_x L_y}{\Delta}\lambda_{qx} + \frac{R_x L_m}{\Delta}\lambda_{qy} - \omega_e\lambda_{dx} \\ V_{dx} + \omega_e\lambda_{qx} + \left[\frac{R_y f L_m'}{\Delta'} - \frac{R_x + R_y f}{\Delta'}\right]\lambda_{dx} + \left[\frac{(R_x + R_y f)L_m' - R_y f L_x'}{\Delta'}\right]\lambda_{dy} \\ \frac{R_y L_m}{\Delta}\lambda_{qx} - \frac{R_y L_x}{\Delta}\lambda_{qy} - \omega_{sl}\lambda_{dy} \\ \left[\frac{R_y(1+f)L_m'}{\Delta} - \frac{R_y f L_y'}{\Delta'}\right]\lambda_{dx} + \omega_{sl}\lambda_{qy} + \left[\frac{R_y f L_m'}{\Delta'} - \frac{R_y(1+f)L_x'}{\Delta'}\right]\lambda_{dy} \end{bmatrix} \tag{49}$$

$$B = \begin{bmatrix} 1 & 0 \\ 0 & 1 \\ 0 & 0 \\ 0 & 0 \end{bmatrix};\ u = \begin{bmatrix} V_{qx} \\ V_{dx} \end{bmatrix};\ h = \begin{bmatrix} \frac{L_y}{\Delta} & 0 & -\frac{L_m}{\Delta} & 0 & 0 \\ 0 & \frac{L_y'}{\Delta'} & 0 & -\frac{L_m'}{\Delta'} & 0 \end{bmatrix} \tag{50}$$

$$F = \begin{bmatrix} -\frac{R_x y}{\Delta} & -\omega_e & \frac{R_x L_m'}{\Delta} & 0 & 0 \\ \omega_e & \frac{R_y f L_m' - (R_x + R_y f)L_y'}{\Delta'} & 0 & \frac{(R_x + R_y f)L_m' - R_y f L_x'}{\Delta'} & A_{25} \\ \frac{R_y L_m}{\Delta} & 0 & -\frac{R_y L_x}{\Delta} & -\omega_{sl} & \lambda_{dy} \\ 0 & \frac{R_y(1+f)L_m' - R_y f L_y'}{\Delta'} & \omega_{sl} & \frac{R_y f L_m' - R_y(1+f)L_x'}{\Delta'} & A_{45} - \lambda_{qy} \\ k_t\left[\left(\frac{L_y}{\Delta} - \frac{L_y'}{\Delta'}\right)\lambda_{dx} + \frac{L_m'}{\Delta'}\lambda_{dy}\right] & k_t\left[\left(\frac{L_y}{\Delta} - \frac{L_y'}{\Delta'}\right)\lambda_{qx} - \frac{L_m}{\Delta}\lambda_{qy}\right] & k_t\left[-\frac{L_m}{\Delta}\lambda_{dx}\right] & k_t\left[\frac{L_m'}{\Delta'}\lambda_{qx}\right] & A_{55} \end{bmatrix}$$

$$H = \begin{bmatrix} \frac{L_y}{\Delta} & 0 & -\frac{L_m}{\Delta} & 0 & 0 \\ 0 & \frac{L_y'}{\Delta'} & 0 & -\frac{L_m'}{\Delta'} & C_{25} \end{bmatrix} \quad (52)$$

References

[1] Kang G, Nam K (2005) "Field-Oriented Control Scheme for Linear Induction Motor with the End Effect", IEE Proceedings Electric Power Application, Vol.152, Iss.6, pp.1565-1572, 2005.

[2] Jeng LF, Tao TL, Kai CC, "Adaptive Back Stepping Control for Linear Induction Motor Drive Using FPGA", Proceeding of the 32nd IECON, Vol.2, Iss.6, pp.1269-1274, 2006.

[3] Silva EFD, Santos CCD, Nerys JWL, "Field Oriented Control of Linear Induction Motor Taking into Account End-Effect", Proceeding of the 8th IEEE-AMC, pp.689-694, 2004.

[4] Silva EFD, Santos EBD, Machado PC, Oliveria MAAD, "Vector Control for Linear Induction Motor", Proceeding of the IEEE-ICIT, pp.518-523, 2003.

[5] Vaez-Zadeh S, Satvati MR, "Vector Control of Linear Induction Motors with End Effect Compensation", Proceeding of the 8th ICEMS, pp.635-638, 2005.

[6] Doncker RWD, Profumo F, Pastorelli M, Ferraris P "Comparison of Universal Field Oriented (ufo) Controllers in Different Reference Frames", IEEE Trans. on Power Electronics Vol.10, pp.205-213, 1995.

[7] Palma JP, Dente JG, Carvalhal FJ,"A Comparison of Simplified Field Oriented Control Methods for Voltage-Source Induction Motor Drives", Proceedings of the ISIE'03, pp.134-139, 2003.

[9] Doncker RW, Prufumo F, "The Universal Field Oriented Controller Applied to Tapped Stator Winding Induction Motors", Proceeding of the 20th PESC'89, pp.1031-1036, 1989.

[10] Prufumo F, Tenconi, Doncker RW, "The Universal Field Oriented (ufo) Controller Applied to Wide Speed Range Induction Motor Drives", Proceeding of the 22nd PESC'91, pp.681-686, 1991.

[11] HaoBin Z, Bo L, BingGang C ,"Vector Control System of Induction Motor Based on Fuzzy Control Method", Proceeding of the PEITS, pp.136-139, 2008.

[12] Yunhai H, Yuhua W, "Based on Neuron Adaptive Controller for Linear Motor Slip Frequency Vector Control system", Proceeding of the IHMSC, Vol.2, pp.94-98, 2009.

[13] Yang Z, Zhao J, Zheng TQ, "High Performance Vector Control of Linear Induction Motors Using Single Neuron Controller", Proceeding of the 4th ICNC '08, pp.534-538, 2008.

[14] Madadi Kojabadi H, Ghribi M, "Sensorless Control of Permanent Magnet Synchronous Motor-a Survey", Proceeding of the VPPC '08, pp.1-8, 2008.

[15] Darabi A, Salahshoor K, "EKF and UKF-Based Estimation of a Sensor-Less Axial Flux PM Machine Under an Internal-Model Control Scheme Using a SVPWM Inverter" Proceeding of the 29th CCC, pp.5676-5681, 2010.

[16] Boussak M, "Implementation and Experimental Investigation of Sensorless Speed Control with Initial Rotor Position Estimation for Interior Permanent Magnet Synchronous Motor Drive", IEEE Trans. on Power Electron., Vol.20, pp.1413–1422, 2005.

[17] Wenqiang Y, Shuguang Li, "Speed Sensorless Vector Control Induction Motor Based on Reduced Order Extended Kalman Filter", Proceeding of the 5th PEDS, pp.1-11, 2003.

[18] Duncan J, "Linear Induction Motor-Equivalent Circuit Model", IEE Electr. Power Appl., Vol.130, Iss.1, pp.51-57, 1983.

[19] Bose BK," Modern power electronics and AC drives", Prentice-Hall press, 2002.

[20] Darabi A, Salahshoor K, "EKF and UKF-based Estimation of a Sensor-Less Axial Flux PM Machine Under an Internal-Model Control Scheme Using a SVPWM Inverter", Proceeding of the 29th CCC, pp.5676-5681, 2010.